Corrosion Science 53 (2011) 513–522

Contents lists available at ScienceDirect

Corrosion Science

journal homepage: www.elsevier.com/locate/corsci

# Critical pitting temperature (CPT) assessment of 2205 duplex stainless steel in 0.1 M NaCl at various molybdate concentrations

F. Eghbali [a], M.H. Moayed [a,*], A. Davoodi [b], N. Ebrahimi [a]

[a] Metallurgical and Material Engineering Department, Faculty of Engineering, Ferdowsi University of Mashhad, Mashhad 91775-1111, Iran
[b] Materials Engineering Department, Faculty of Engineering, Sabzevar Tarbiat Moallem University, Sabzevar 391, Iran

ARTICLE INFO

*Article history:*
Received 21 May 2010
Accepted 8 August 2010
Available online 11 August 2010

*Keywords:*
A. Stainless steel
B. Polarisation
C. Passivity
C. Pitting corrosion

ABSTRACT

In this study, the influence of various concentrations of molybdate ($MoO_4^{2-}$) on critical pitting temperature (CPT) of duplex stainless steel 2205 (DSS 2205) in 0.1 M NaCl solution has been investigated by employing potentiodynamic and potentiostatic CPT measurements methods. No significant increase in CPT was observed in the presence of 0.0001 and 0.001 M molybdate. However, addition of 0.01 M $MoO_4^{2-}$ increases 10 °C in CPT and pitting corrosion was not observed in solution containing 0.1 M molybdate up to 85 °C. Potentiostatic CPT measurements showed CPT values of 68 and more than 85 °C in 0.01 and 0.1 M molybdate concentrations, respectively.



## 1. Introduction

Duplex stainless steels (DSS) having two-phase of austenite–ferrite microstructure have been paid attention owing to their outstanding corrosion and mechanical properties in various applications such as petroleum, gas refineries and marine environments [1–9]. However, corrosion control is an essential issue from application point of view and it has been reported that inhibitors are needed to be used which act as a barrier to reduce the aggressiveness of the environments against the pitting corrosion attack against stainless steel [3,4,10–14] including DSS [3,4].

The use of molybdate as an inhibitor has been studied for a long time [15,16] for inhibition of mild steel pitting corrosion [13,14], 304 and 316 stainless steel [11] and Fe–18Cr alloys [12]. Although some unidentified issues regarding the exact mechanism of molybdate corrosion inhibition are still remained, but the general presume is that molybdate ion affects both the nucleation of metastable and the stable pitting by reducing the numbers and sizes of pit events on the metal surface especially at the sites of inclusions. Molybdate ion blocks the reactive site on the surface and reduces the local acidity at site where they react [12]. Tobler et al. reported that molybdate ions decrease the number and magnitude of single current transient observed in the passive region below the pitting potential. Refaey et al. [13,14] also state that the presence of inorganic molybdate ions prevents pitting corrosion both in sodium chloride and acidified solution by increasing the pitting potential to the more noble values.

Critical pitting temperature (CPT) defines the lowest potential-independent temperature, below which pitting does not occur [2,5,17–19]. The principal advantage of the test is the rapidity with which the CPT can be measured in a single test. Effect of sulphate, $SO_4^{2-}$ and ion concentration on CPT in $Cl^-$-containing solutions revealed an accelerating and inhibiting effect of low and high concentrations of $SO_4^{2-}$ ion, respectively, on pitting initiation based on the mechanism of ions-competitive adsorption between $SO_4^{2-}$ and $Cl^-$ ions [21]. The addition of sulphate to NaCl solution stabilizes pit growth despite the increase in pitting potential [22]. $SO_4^{2-}$ ions can lower the CPT by promoting pits growth over the range of potentials below that normally used for CPT evaluation. The lacy metal that covers over the pit has a finer pore structure with sulphate present, because passivation is easier in the pit solution [23,24]. However, to date, studies focusing on the inhibiting effect of molybdate on pitting corrosion and particularly CPT of 2205 DSS in $Cl^-$-containing solutions are rarely reported. In the present research, by utilizing microscopic examination, potentiodynamic and potentiostatic polarisation and standard CPT measurements, the beneficial influence of molybdate ion on 2205 DSS in 0.1 M NaCl, will be discussed.

## 2. Materials and experimental methods

The specimens were 2205 DSS plates with 30 mm thickness and chemical composition analysis of (in wt.%) 0.03% C, 0.97% Mn, 0.022% P, 0.0007% S, 0.74% Si, 21.61% Cr, 5.31% Ni, 3.07% Mo, 0.16% Cu, 0.22% N, 0.136% V, 0.064% W, 0.01% Ti and Fe balance, in agreement with the UNS S31803 (AISI 2205). Two types of

* Corresponding author. Tel./fax: +98 511 8763305.
*E-mail address:* mhmoayd@um.ac.ir (M.H. Moayed).

0010-938X/$ - see front matter © 2010 Elsevier Ltd. All rights reserved.
doi:10.1016/j.corsci.2010.08.008

sample cross sections have been prepared. The first one was cut into a rod shape with 10 mm in diameter and hemisphere ended. The immersion depth of the working electrode was 10 mm and the immersion surface area was ca. 3.2 $cm^2$. It has been tried to have at least 3.2 $cm^2$ immersion surface area in each CPT measurement as shown in Fig. 1. Orientation of the long axis of working electrodes was parallel to the rolling direction. Preparing such a shape of samples avoids any crevice corrosion during pitting corrosion measurements. To minimize the water-line attack, the solution was deaerated for 80 min before starting the test. Therefore, the local effects of water-line attack were minimized [25]. To be even more on the safe side, after each experiment, the specimen was examined by stereo microscope and no water-line attack was observed. In addition to this type of samples, the second type of specimens was prepared as flat samples with $1 \times 1$ $cm^2$ surface area for pit morphology observation. In potentiostatic polarisation measurements to accentuate the current fluctuations in passivity region, flat samples with smaller surface area ($0.5 \times 0.5$ $cm^2$) also have been used. To avoid crevice corrosion, all specimens were prepassivated in 65% $HNO_3$ at 70–80 °C for 1 h, rinsed by water and methanol, dried by hot air and then mounted in self-cure acrylic. Although later grinding of the surface with silicon carbide paper destroys the protective layer of surface, it does not destroy the passive layer of the mounted faces of specimen. For more accuracy, the interface between sample and mount was checked by stereo microscope and no crevice was observed. Before polarisation tests, all samples were ground up to 600 SiC paper and then degreased in ultrasonically cleaned acetone for 5 min prior to washing with distilled water. A similar preparation was performed on a specimen with a finishing surface of 0.3 μm diamond paste for microscopy observation.

ACM potentiostat (ACM Instruments) was employed for the electrochemical three electrode tests including working, reference and counter electrodes. For reference and counter electrodes, saturated calomel and platinum wire with a surface area of 2 $cm^2$ were chosen, respectively. All tests related to pitting potential and CPT evaluations were performed in 0.1 M NaCl and 0.1 M NaCl plus 0.0001, 0.001, 0.01 and 0.1 M $MoO_4^{2-}$ solutions in various temperatures. The pH of the solution was 5.9 and it was measured by Inolab pH meter. In all measurements, the electrolyte in the cell was deaerated with purified nitrogen gas for 80 min before the test and purging was continued above the electrolyte until the end of experiments as shown schematically in Fig. 2. During the nitrogen gas purging, working electrode was held above the electrolyte. Each test was repeated at least three times to ensure reproducibility.

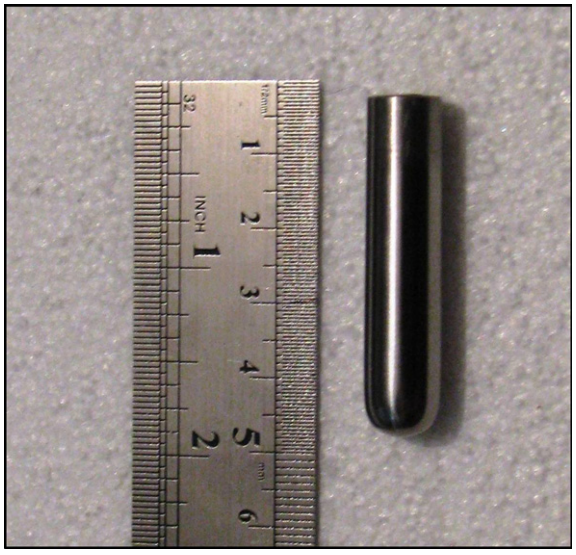


**Fig. 1.** Hemisphere end sample prepared for potentiodynamic tests and CPT assessment.

Potentiodynamic polarisation measurement was carried out at various temperatures to obtain the breakdown potential. Before polarisation measurements, open circuit potential was measured for 60 min to stabilize the rest potential. The scan rate was 1 mV/s (1000 and 2000 data points for high and low temperatures, respectively) sweeping from 50 mV cathodic potential up to the potential value at where a sudden current density, about 0.1 mA/$cm^2$, increasing due to extensive pitting corrosion or transpassivity, had occurred. Breakdown potential, $E_b$, was identified as the potential where the current density continuously exceeded 100 μA/$cm^2$. To obtain the passivity current density in the passivity domain, potentiostatic measurements were also performed in the anodic potential of 850 mV versus OCP (ca. 480 mV SCE) at various temperatures. The aim was to characterize the passive layer integrity and examine the metastable pitting. It should be noted that OCP values may change with temperature and molybdate concentration. However, 850 mV anodic potential versus OCP was chosen to situate relatively the identical driving force for all samples.

All potentiostatic CPT measurements were carried out at applied anodic potential of 750 mV versus corrosion potential (ca. 380 mV SCE) and the temperature was increased at a rate of 0.6 °C/min until the current density exceeds 100 μA/$cm^2$. The temperature associated to this current density was chosen as a criterion for CPT assessment. It should be noted that the real steady state conditions during potentiostatic tests do not achieve completely in short time measurements and it takes at least several hours [26]. However, comparative examination of the samples after 900 s could be performed.

For microstructure examination of alloy, the as-received alloy was ultrasonically cleaned and then washed with alcohol, dried and electroetched in 4 M NaOH solution at 25 °C, at 2 V DC applied potential for about 30 s. To evaluate the morphology of stable and metastable pits in various temperatures, potentiostatic measurements were carried out with 850 mV anodic potential versus OCP (ca. 480 mV SCE) in the range of passivity. Five data per second were recorded during potentiostatic measurements. A mirror-like surface was prepared by grinding the sample up to 1200 SiC papers followed by polishing with 0.3 μm diamond paste. Microscopical examination of pitting morphology also performed on the samples after their anodic polarisation was beyond the pitting potential. A Kalling's number 2 reagent was used as an etchant. Metallographic examination was carried out using optical microscope and scanning electron microscope (SEM).

## 3. Results and discussion

### 3.1. Microstructure evaluation

Fig. 3 shows the microstructure of 2205 DSS which demonstrates 53–47% austenite–ferrite microstructure phases elongated in the rolling direction after the annealing step. The interface between the two-phases has been clearly etched, as shown in Fig. 3, and the island-like austenite phase (light regions) was embedded in the continuous ferrite matrix (dark regions) [1,2,4].

### 3.2. Potentiodynamic measurements

Potentiodynamic polarisation curves of 2205 DSS alloy in 0.1 M NaCl at different temperatures are shown in Fig. 4 (In order to compare the results here with Fig. 5, the inserted graph shows the polarisation curves also in E-i format). Generally, by increasing the temperature from 25 to 85 °C, the passivity current increases

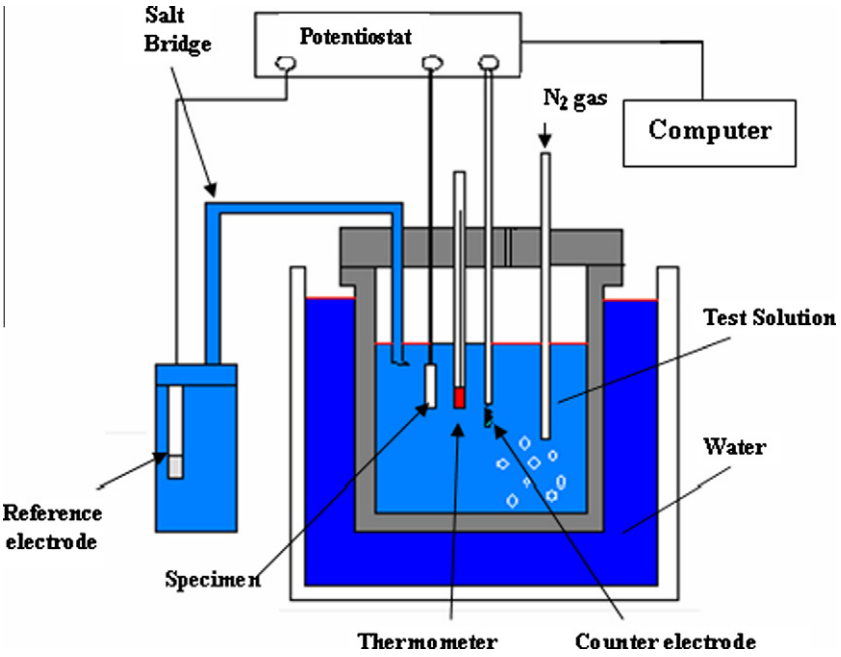


**Fig. 2.** Schematic of the electrochemical cell used in corrosion tests.

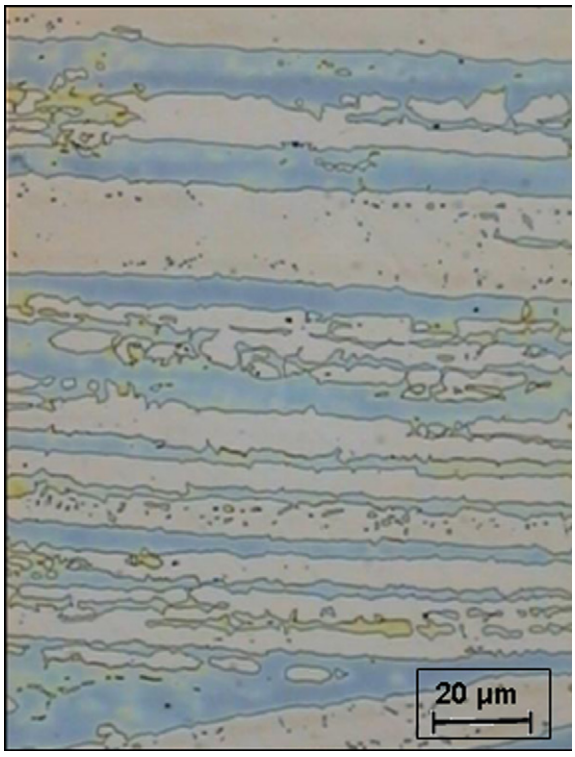


**Fig. 3.** Microstructure DSS 2205 showing ferrite (dark region) and austenite (light region) phases and interface between them.

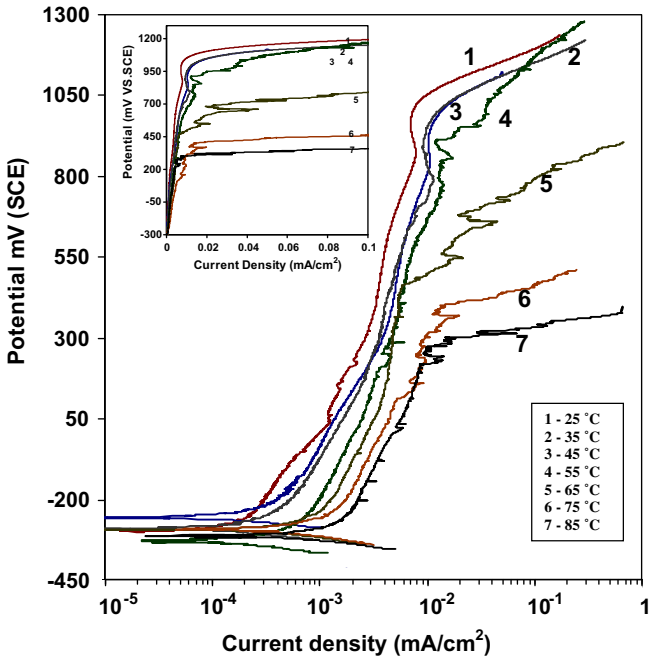


**Fig. 4.** Potentiodynamic polarisation curves of DSS 2205 in 0.1 M NaCl at different temperatures. Scan rate was 1 mV/s. To compare the results here with Fig. 5, the inserted graph shows the polarisation curves in E-i format.

from 1.1 to 6.5 μA/cm$^2$, which is more noticeable at a higher temperature. Moreover, it can be observed that in 0.1 M NaCl, in the temperature range from 25 to 55 °C, the alloy shows passivity which is extended up to more than ca. 1100 mV prior to dissolution by transpassivity, similar to the results reported previously in 3.5% NaCl solution [7]. Up to 55 °C, a passivity domain of about 1350 mV (from OCP to breakdown potential) was obtained. At 55 °C, a slight increase of current density fluctuations in passivity domain is observed and by increasing the temperature to 65 °C, a transition from transpassivity to pitting corrosion is occurred; see Fig. 4. Based on the potential associated to 100 μA/cm$^2$ as the criterion for the breakdown potential, the pitting potential of ca. 790 mV at 65 °C is observed and the passivity domain is decreased from 1350 mV at 45 °C to 1040 mV at 65 °C (Further increasing the temperature results in more decrease in the pitting potential to 440 and 330 mV at 75 and 85 °C, respectively). Generally, decrease in the pitting potential is a combined effect of chloride concentration and temperature [10,19]. A value of 400 mV has been reported

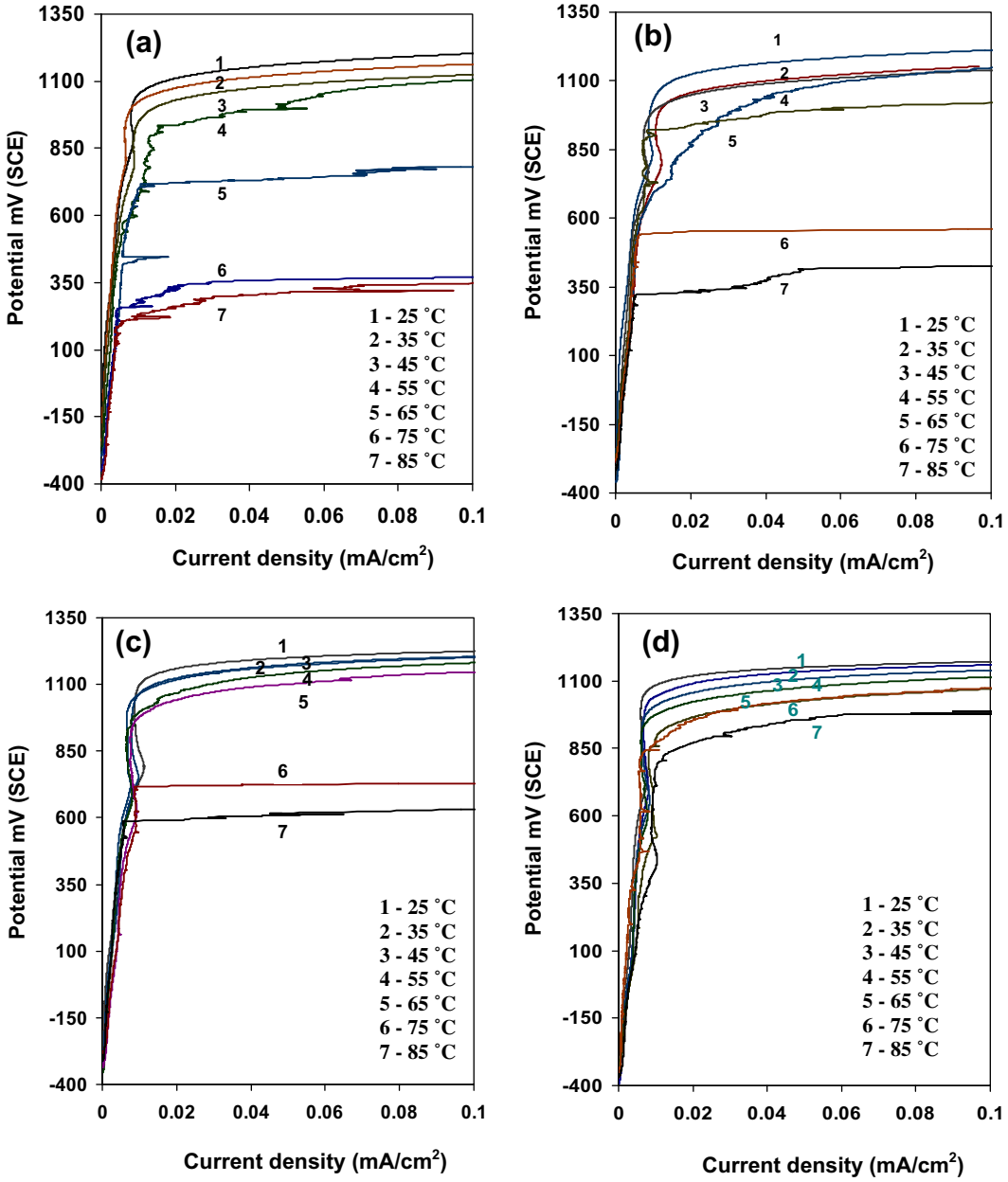


**Fig. 5.** Potentiodynamic polarisation curves of DSS 2205 in 0.1 M NaCl with (a) 0.0001 M, (b) 0.001 M, (c) 0.01 M and (d) 0.1 M $MoO_4^{2-}$ at different temperatures. Scan rate was 1 mV/s.

previously for the breakdown potential at 60 °C in 3.5% NaCl [7]. In the present study, a value of 790 mV at 65 °C was obtained in 0.1 M NaCl which confirms that the breakdown potential depends upon both temperature and the chloride concentration. In summary, based on the potentiodynamic measurements at various temperatures, shown in Fig. 4, in 2205 DSS alloy, a transition from transpassivity to pitting corrosion occurs between 55 and 65 °C in 0.1 M NaCl solution.

Potentiodynamic results of the alloy in 0.1 M NaCl plus 0.0001, 0.001, 0.01 and 0.1 M $MoO_4^{2-}$ at different temperatures are shown in Fig. 5. Generally, the influence of adding molybdate ions on breakdown potential in the temperature range of 25–55 °C is insignificant. This means that in the temperature range of 25–55 °C, a passivity domain of about more than 1350 mV (from OCP to breakdown potential) was obtained and the transpassivity occurred at higher potentials. A slight increase in transpassivity breakdown potential by adding 0.01 M molybdate is observed. By further increasing the temperature, a significant decrease in breakdown potential is observed which is associated to pitting occurrence. But adding molybdate to the solution shows different behaviour at high temperature. This can be seen more clearly in Fig. 6 where the breakdown potential of 2205 DSS obtained in Fig. 5 has been plotted against temperature. At the lowest concentration, 0.0001 M $MoO_4^{2-}$, an inverse influence is observed wherein by the addition of inhibitor a further decrease in the pitting potential is observed. Improving the pitting potential when the concentration of the inhibitor reaches to 0.001 M may address that the beneficial inhibitor concentration should be in between 0.0001 and 0.001 M $MoO_4^{2-}$. Further increasing the molybdate concentration to 0.01 and 0.1 M results in an even more improvement in the pitting potential. Particularly, in 0.1 M $MoO_4^{2-}$, the breakdown potential is increased significantly and reached to the transpassivity even at temperature 85 °C, see Fig. 6. This means that the pitting corrosion does not occur in 0.1 M NaCl + 0.1 M $MoO_4^{2-}$ even at the highest recorded temperature,

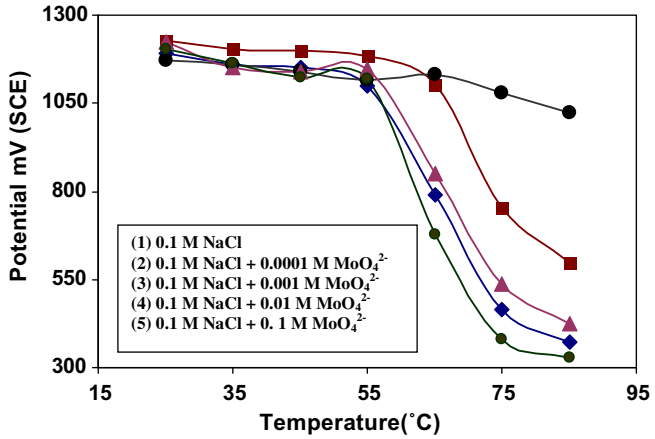


**Fig. 6.** Evaluation of breakdown potential for 2205 DSS based on the results in Fig. 5. A 100 μA/cm$^2$ was chosen.

85 °C. Increasing the breakdown potential due to adding $MoO_4^{2-}$ can be associated to reducing the numbers and the magnitude of metastable pitting transients on the two-phase microstructure 2205 DSS alloy surface. This means that molybdate ions block the active site on the surface [10] and decrease significantly the metastable pitting current transient. Reduction of the number and magnitude of metastable pits by increasing molybdate content has been investigated previously [10]. Mo as an alloying element in 2205 DSS also decreases the transient height where Mo can be dissolved at local activation site reacting directly in the aggressive pit environment. Therefore, the repassivation of metastable pit is enhanced and the growth of stable pit is hindered [12]. As a result, the pitting potential is increased to the more noble values. It seems that the mechanisms of effecting alloying Mo and effecting molybdate on pitting corrosion resistance are very similar, but not exactly the same. However, comparison between molybdenum as an alloying element and molybdate as a solution constituent has been investigated previously [10,15,27,28]. Fig. 7 shows the cyclic potentiodynamic polarisation curve of DSS 2205 in 0.1 M NaCl in 65 °C and 0.1 M NaCl + 0.1 M $MoO_4^{2-}$ at 85 °C. Clearly, without inhibitor, the alloy

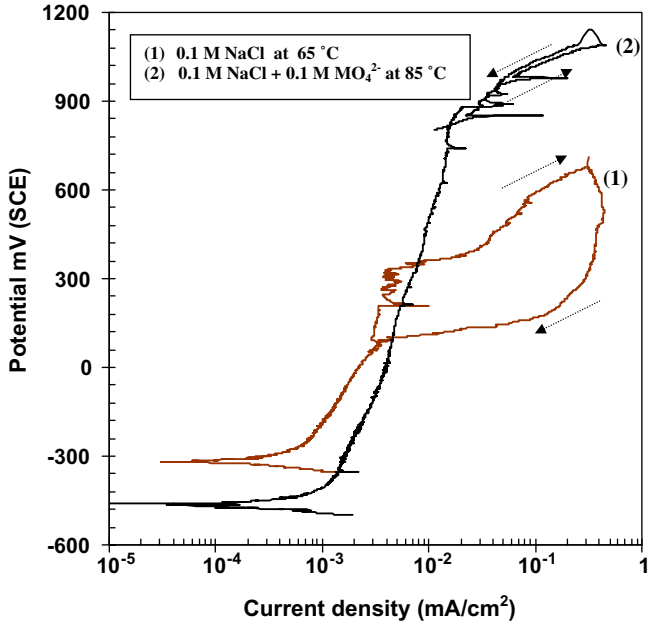


**Fig. 7.** Cyclic potentiodynamic polarisation curves of DSS 2205 in 0.1 M NaCl in 65 °C and 0.1 M NaCl + 0.1 M $MoO_4^{2-}$ in 85 °C.

exhibits a hysteresis loop at 65 °C, indicating that repassivation of existing pits is more difficult when the potential is swept toward the negative direction. However, by adding the inhibitors, forward and backward potentiodynamic scans are the same with negligible hysteresis loop indicating a transpassivity characteristic of passivation breakdown [4].

Since pitting occurs only at high temperature, in Fig. 8, the pitting potential has been plotted against the logarithm of inhibitor concentration. Up to 0.01 M $MoO_4^{2-}$, a linear relationship can be extracted between the pitting potential and the logarithm of $MoO_4^{2-}$ concentration which is in agreement with previous statement [10] and the results of inhibiting effect of $MoO_4^{2-}$ on the potting corrosion of mild steel in HCl solution [13]. In another study, the dependence of the pitting potential of mild steel in 0.1 M NaCl on the concentration of $MoO_4^{2-}$ inorganic salts has been investigated and the results showed a nonlinear relationship between them [14]. Even further, pitting potential decreases controversially by increasing $MoO_4^{2-}$ close to 0.1 M. No explanation has been stated in the paper [14]. Noticeably, in the present study, further adding of 0.1 M $MoO_4^{2-}$ at 65 °C has less beneficial influence than adding 0.01 M $MoO_4^{2-}$.

In summary, at room temperature up to 65 °C, the most advantageous $MoO_4^{2-}$ concentration as the satisfactory inhibitor is ca 0.01 M whereas at high temperature of more than 65 °C, the optimum $MoO_4^{2-}$ concentration is 0.1 M. Generally, the beneficial effect of inhibitor is more enhanced at high temperature.

To elucidate the influence of adding molybdate ion on passive current density, potentiodynamic polarisation curve of DSS 2205 in 0.1 M NaCl and 0.1 M NaCl + 0.01 M $MoO_4^{2-}$ at 75 °C has been plotted as shown in Fig. 9. The results reveal that the highest passivity current density is associated to the 0.1 M NaCl solution and adding $MoO_4^{2-}$ decreases the passivity current density from 0.007 to 0.002 mA/cm$^2$. Noticeably, the passivity current is not substantially reduced by adding molybdate inhibitors which is in contrast with previous report on 314 and 316 austenitic stainless steel in HCl [10]. This means that the passivity integrity and stability of the two-phase microstructure 2205 DSS do not improve extensively in the presence of molybdate inhibitor.

### 3.3. Potentiostatic polarisation measurements

Passivity current density as a criterion for passivity integrity was characterized at various temperatures and inhibitor

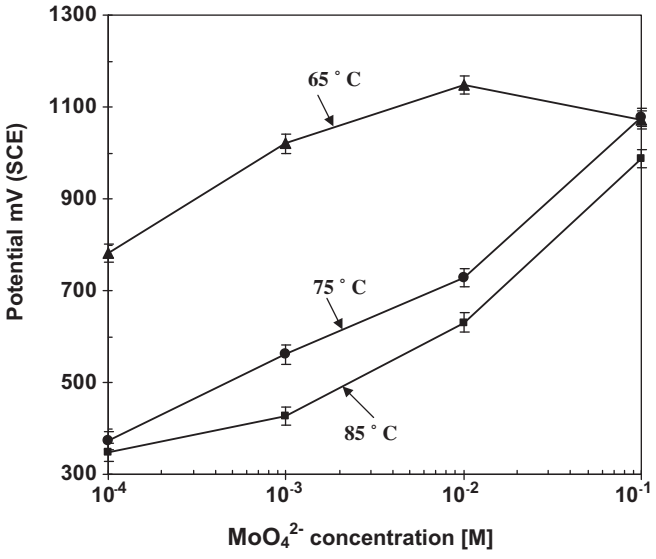


**Fig. 8.** Pitting potential versus logarithm of $MoO_4^{2-}$ inhibitor concentration.

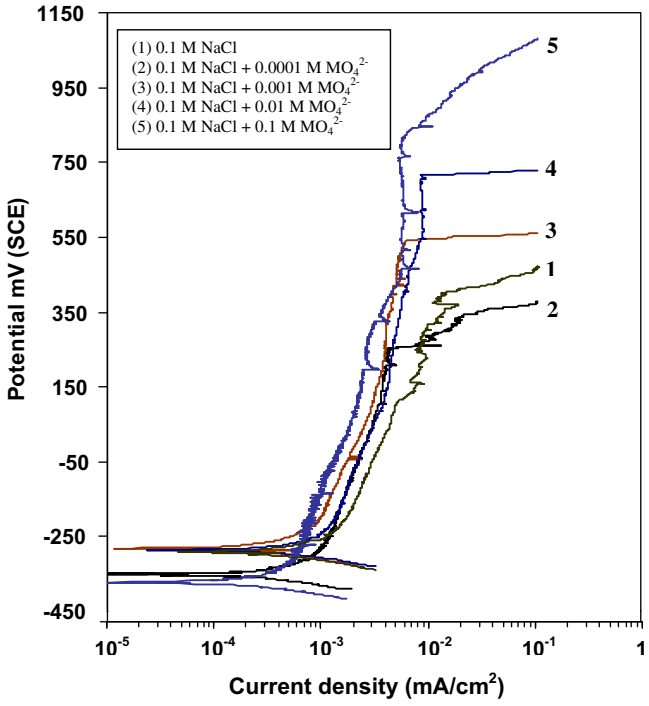


**Fig. 9.** Potentiodynamic polarisation curves of DSS 2205 in 0.1 M NaCl and 0.1 M NaCl plus 0.0001, 0.001, 0.01 and 0.1 M $MoO_4^{2-}$ at 75 °C. Scan rate was 1 mV/s.

concentrations. In order to be able to record the metastable pitting current transients in the presence of molybdate as an inhibitor anion on a high alloy 2205 duplex stainless steel, a relatively high anodic potential was selected. As an example, Fig. 10 shows the results with applying 850 mV anodic potential with respect to OCP (480 mV/SCE) in 2205 DSS at various temperatures in 0.1 M NaCl and 0.1 M NaCl + 0.01 M $MoO_4^{2-}$. The current density in 0.1 M NaCl solution decreases within the time and lies down in the passivity domain up to the temperature 50 °C. However, by increasing the temperature to 60 °C, the current density increases up to 2 mA/cm$^2$ after 900 s (the inserted graph) indicating the presence of stable pitting occurred on the sample surface. Moreover, by increasing the temperature, the passivity current density increases and more current fluctuations were observed which can be associated to the metastable pits creation on the surface, particularly at the temperature 50 °C. However, increasing the background passivity current hides the current fluctuations at higher temperatures; see Fig. 10a. Previous results [2] on 2205 DSS showed that in 1 M NaCl, the transition from transpassivity to pitting occurred in between 56 and 63 °C which is similar to the present results (note that the chloride concentration here is 0.1 M). On the other hand, considering the results in 0.1 M NaCl + 0.01 M $MoO_4^{2-}$ solution in Fig. 10b, it can be seen that the current density decreases within the time and lies down in the passivity domain up to temperature 80 °C, but by further increasing the temperature to 85 °C, the current density increases up to 2 mA/cm$^2$ after 900 s (the inserted graph) indicating occurrence of the stable pitting on the sample surface. This means that molybdate ion increases the transition temperature from passivity to pitting by more than 20 °C in potentiostatic measurements. Moreover, by adding the inhibitor the passivity current density was decreased at a comparable temperature in 0.1 M NaCl and 0.1 M NaCl + 0.01 M $MoO_4^{2-}$. As an example, the passivity current density at 50 °C was decreased four times (from 0.004 to 0.001 mA/cm$^2$), see Fig. 10b. Similar to previous results in Fig. 10a, increasing the temperature enhanced the passivity current density and current fluctuations associated to the metastable pits created on the surface, particularly in the temperature above 60 °C covered by the higher background passivity current at higher temperatures.

Similar measurements were also obtained for other $MoO_4^{2-}$ concentrations indicating that in 0.1 M $MoO_4^{2-}$, the passivity prolongs up to temperature 85 °C. The results revealed that at 85 °C, after 300 s, the current densities of 9.37, 0.49, 0.22 and 0.005 mA/cm$^2$ in 0.0001, 0.001, 0.01 and 0.1 M $MoO_4^{2-}$, respectively, were obtained indicating that by increasing molybdate ions, the current density decreases reached to passivity level (0.005 mA/cm$^2$). Noticeably, the current density in 0.1 M NaCl without inhibitor was about 6.755 mA/cm$^2$ which is less than the solution containing 0.0001 M $MoO_4^{2-}$ (9.37 mA/cm$^2$).

In summary, potentiostatic polarisation measurements confirm the potentiodynamic results on the beneficial influence of adding optimum molybdate ions on improving pitting corrosion resistance by decreasing passivity current density.

### 3.4. Potentiostatic CPT measurements

Fig. 11 represents the results on evaluation of CPT in 2205 DSS with potentiostatic measurement by applying 750 mV anodic potential (ca. 380 mV SCE) and gradually increasing the temperature. Considering 100 μA/cm$^2$ current density as a criterion for CPT evaluation, it can be seen that adding 0.0001, 0.001 and 0.01 M $MoO_4^{2-}$ increases CPT to about 0.5, 2.5 and 12 °C, respectively (from 73 °C in 0.1 M NaCl to 85 °C in 0.1 M NaCl + 0.01 M $MoO_4^{2-}$). Noticeably, no CPT value could be reported by adding 0.1 M $MoO_4^{2-}$ up to 86 °C. A CPT of ca. 60 °C was obtained previously for 2205 DSS in 1 M NaCl [2]. Here, in 0.1 M NaCl, the CPT was 73 °C and it has been improved to 85 °C by adding 0.01 M $MoO_4^{2-}$.

CPT-assessed values have been plotted against logarithm of inhibitors concentration as represented in Fig. 12. Clearly, the inhibiting efficiency of $MoO_4^{2-}$ is enhanced from 0.001 to 0.01 M $MoO_4^{2-}$ by the sudden increase in CPT from 75.5 to 85 °C. It has been previously stated that at a constant concentration of aggressive ion, $Cl^-$, there exists a linear relationship between the pitting potential and the logarithm of inhibitors concentration [10], i.e. pitting potential should linearly increase by increasing the inhibitor concentration. However, no relationship has been reported yet between inhibitor concentrations and the CPT values. According to Fig. 12, a nonlinear relationship could fit the CPT increase as a function of log $MoO_4^{2-}$ concentration. Further study with various interval concentrations is needed to extract the exact relation. However, in this paper, for the first time, the positive effect of $MoO_4^{2-}$ on CPT of 2205 DSS has been reported. The effect of $MoO_4^{2-}$ ion on CPT in $Cl^-$-containing solutions revealed a negligible positive effect at significantly low $MoO_4^{2-}$ concentration. At higher enough $MoO_4^{2-}$ concentrations, more than 0.01 M, molybdate reveals clearly an inhibiting effect by increasing CPT values. A mechanism of ions-competitive adsorption between $MoO_4^{2-}$ and $Cl^-$ ions in NaCl solution on alloy surface has been proposed previously [23,24]. In addition, the inhibitive nature of molybdate anion may be due to the formation of a thin film of molybdate ion itself. With increase in molybdate concentration, the fraction of Mo as $Mo^{4+}$ is decreased due to its limited solubility and sufficient amount of $MoO_4^{2-}$ adsorbs on the surface forming a thin molybdate salt layer. As a result, diffusion of aggressive $Cl^-$ will be restricted by the presence of this salt film leading to a higher pitting potential and most likely a higher CPT values. $MoO_4^{2-}$ absorbed on the oxide surface through hydrogen bonding between the hydrogen atom of the hydroxyl group of the oxide and the oxygen atom of the molybdate ion. This makes the surface repels aggressive $Cl^-$ [13,14]. In another study, the inhibiting influence of alloying with Mo element was addressed to retard the active dissolution with no salt film

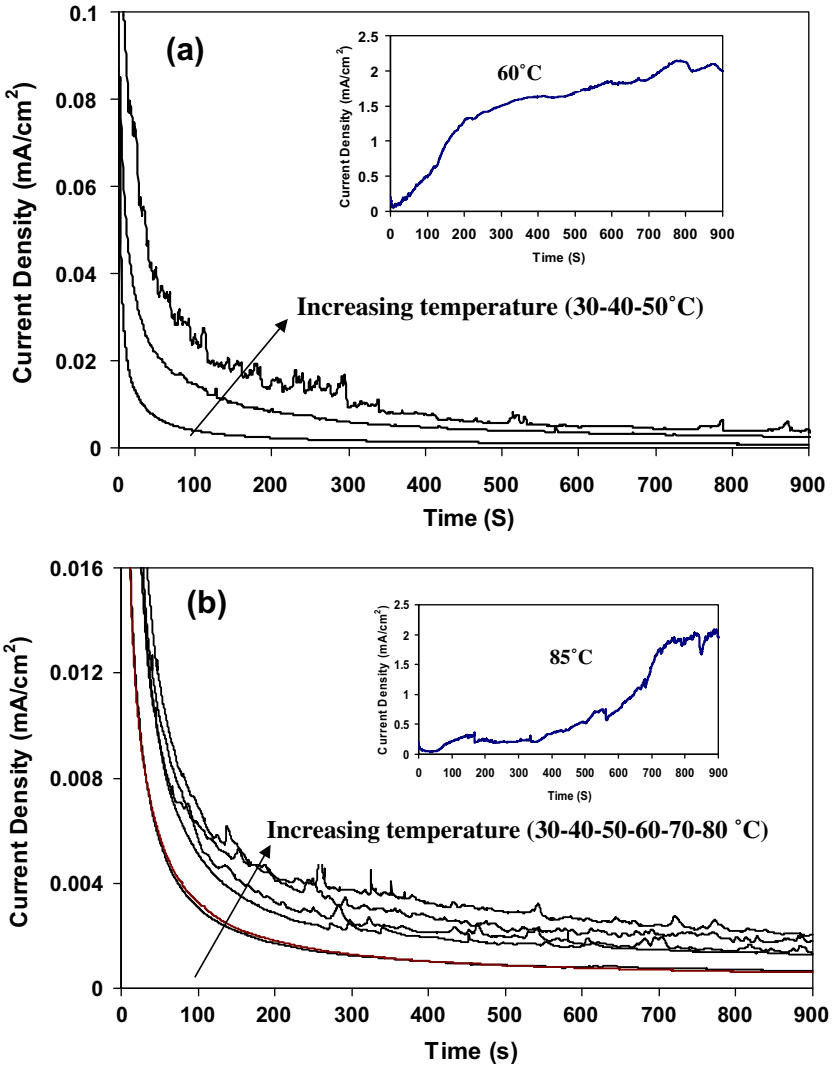


**Fig. 10.** Potentiostatic polarisation results with applying 850 mV anodic potential with respect to OCP in 2205 DSS in various temperature in (a) 0.1 M NaCl and (b) 0.1 M NaCl + 0.01 M $MoO_4^{2-}$.

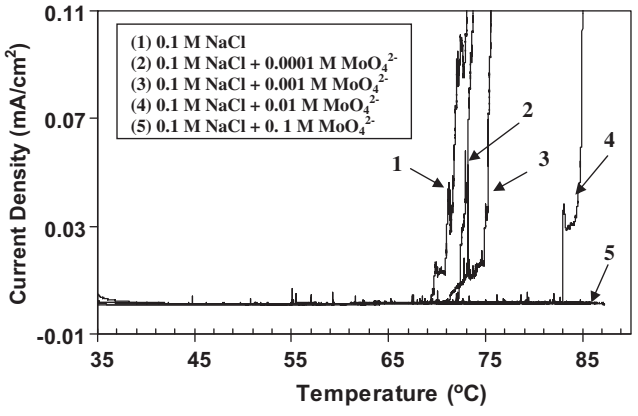


**Fig. 11.** Evaluation of CPT in 2205 DSS with potentiostatic measurement at anodic potential and temperature increasing rate of 750 mV and 0.6 °C/min, respectively.

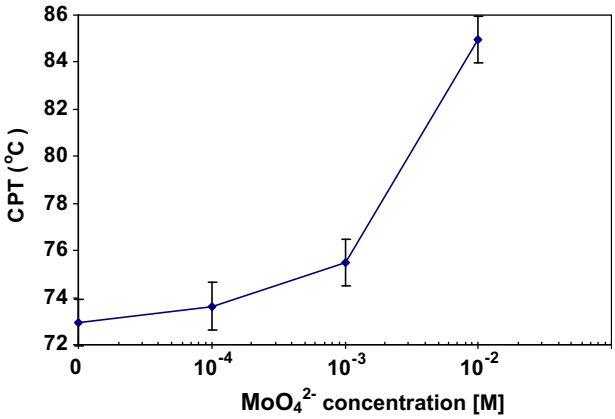


**Fig. 12.** CPT versus log of inhibitors concentration.

presence, though other interpretations based on the presence of a salt film are also mentioned to be possible [24].

It is known that CPT is related to the transition from metastable to stable pit growth. According to the mechanism proposed by Laycock et al. [29], it can be assumed that all stable pits must develop and maintain an anodic salt and there is a critical current density for passivation in the saturated salt environment of the pit nucleus, $i_{crit}$ which increases with temperature. There is also a limiting current density, $i_L$ given by the saturation concentration

of metal ions, $C_S$ and Fick's first law, which increases more gradually with $T$ than $i_{crit}$

$$i_L = n \cdot F \cdot D \cdot C_S / h \quad (1)$$

where $C_S$ is the saturation concentration of salt, $h$ the pit radius, $D$ the diffusivity, $n$ the dissolution valence and $F$ the Faraday constant [29].

The CPT corresponds to the temperature at which $i_{crit} = i_L$ since below this temperature the alloy cannot generate the anodic current density required to maintain the necessary pit chemistry. Any factor which causes $i_{crit}$ to decrease must be compensated by increasing the temperature leading to increase the CPT. An important factor, which might affect the strength of an inhibitor, is the size of the inhibiting species. It was shown that the radii and volumes of $Cl^-$ and $MoO_4^{2-}$ are comparable [10]. It is therefore possible for $MoO_4^{2-}$ ions to be pulled through the oxide film under the influence of an electric field. Therefore, $MoO_4^{2-}$ ions can diffuse into the pit cavity [10].

It is widely accepted that attack of the material by $Cl^-$ causes acidification of the local electrolyte within the pit. When the pH value becomes less than six, polymerisation begins and paramolybdate is formed as follows:

$$7MoO_4^{2-} + 8H^+ \Longleftrightarrow Mo_7O_{24}^{6-} + 4H_2O \quad (2)$$

When the pH falls further, new condensed species are formed:

$$Mo_7O_{24}^{6-} + 3H^+ + HMoO_4^- \Longleftrightarrow Mo_8O_{24}^{4-} + 2H_2O \quad (3)$$

Another possible reaction is following:

$$MoO_4^{2-} + 4H^+ + 2e^- \Longleftrightarrow MoO_2 + 2H_2O \quad (4)$$

Reduction products are believed to be deposited on the metal surface [10,20].

Another explanation for the inhibiting ability of $Na_2MoO_4$ is that they reduce the local acidity at the sites where they react. According to the above-mentioned Eqs. (1), (3), and (4), by reducing $Na_2MoO_4$, $H^+$ ions are consumed and water molecules are produced. Therefore, the low pH environment necessary for pit development is faded away. This would affect the rate of dissolution within the pit cavity and retarding pit stability by eliminating the possibility of $i_{crit} = i_L$, which is the criteria for pit stability suggested by Laycock et al. [29]. This means that to attain the pit stability criteria, one needs to increase the temperature, i.e. higher CPT.

Inhibiting species are only effective above a certain concentration ratio of nonaggressive to aggressive ions when species like $Cl^-$ are present in the solution [3]. The lack of inhibition effect of molybdate ions less than 0.001 M might be attributed to pH changes of the pit environment in which the pH cannot be raised enough to passivate the pit.

Concentration-dependent effect of molybadte inhibitor on CPT can be compared with data available on the effect of alloyed molybdenum. Sugimoto and Sawada [15] showed that a linear relation exists between weight percent of alloyed molybdenum and CPT for austenitic steels containing 20% Cr, 9–20% Ni and 1–5% Mo (CPT (°C) = 20 + 5 × (wt.%) Mo). Recently, Pardo et al. [20] also investigated the effect of alloying Mo on CPT of austenitic stainless steels; they illustrated that by increasing the Mo, CPT value also increased. For instance, in stainless steels with 0.98 wt.% Mn, an increase of Mo content from 0.30 to 2.74 wt.% displaced the CPT values from 41 to 61 °C. In our knowledge, there is no available information on the effect of alloyed molybdenium on CPT of DSS alloys. However, the above results are somewhat comparable to the present findings that increasing molybdate to solution environment also increases the 2205 DSS CPT value.

In summary the results of potentiodynamic, potentiostatic measurements at various temperatures and the results of CPT assessment confirm the beneficial influence of molybdate inhibitor on 2205 DSS pitting corrosion resistance.

### 3.5. Pit observation

Fig. 13 reveals an example of metastable pit morphology of 2205 DSS in 0.1 M NaCl and 0.1 M NaCl + 0.01 M $MoO_4^{2-}$ after applying 850 mV anodic potential with respect to corrosion potential (ca. 480 mV SCE) in a potentiostatic polarisation at 45 °C. A few metastable pits were observed in austenite phase and austenite–ferrite interface which is clearer in Fig. 13b. Fig. 14 also displays stable pit morphology of DSS 2205 after anodic polarisation at the same potential but at 55 °C in 0.1 M NaCl. Again, a cluster of pitting cavities is observed. It seems that the pitting initiated in boundary region between austenite and ferrite which is probably the weakest point on the surface [2] and propagated in austenite phase. This has also been reported previously [30] and recently by Deng et al. [2]. The reason may be associated to chromium

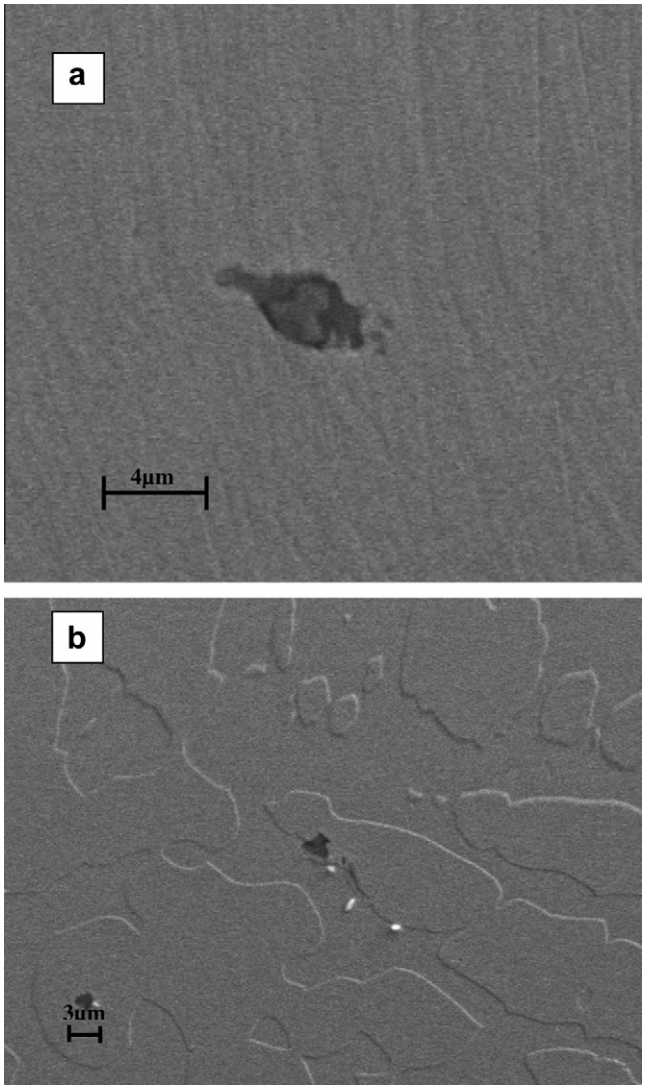


**Fig. 13.** Metastable pit morphology of DSS 2205 (a) in 0.1 M NaCl after 850 mV potentiostatic polarisation above corrosion potential at 45 °C (b) in 0.1 M NaCl + 0.01 M molybdate after dynamic polarisation test with scan rate 3 mV/min at 45 °C.

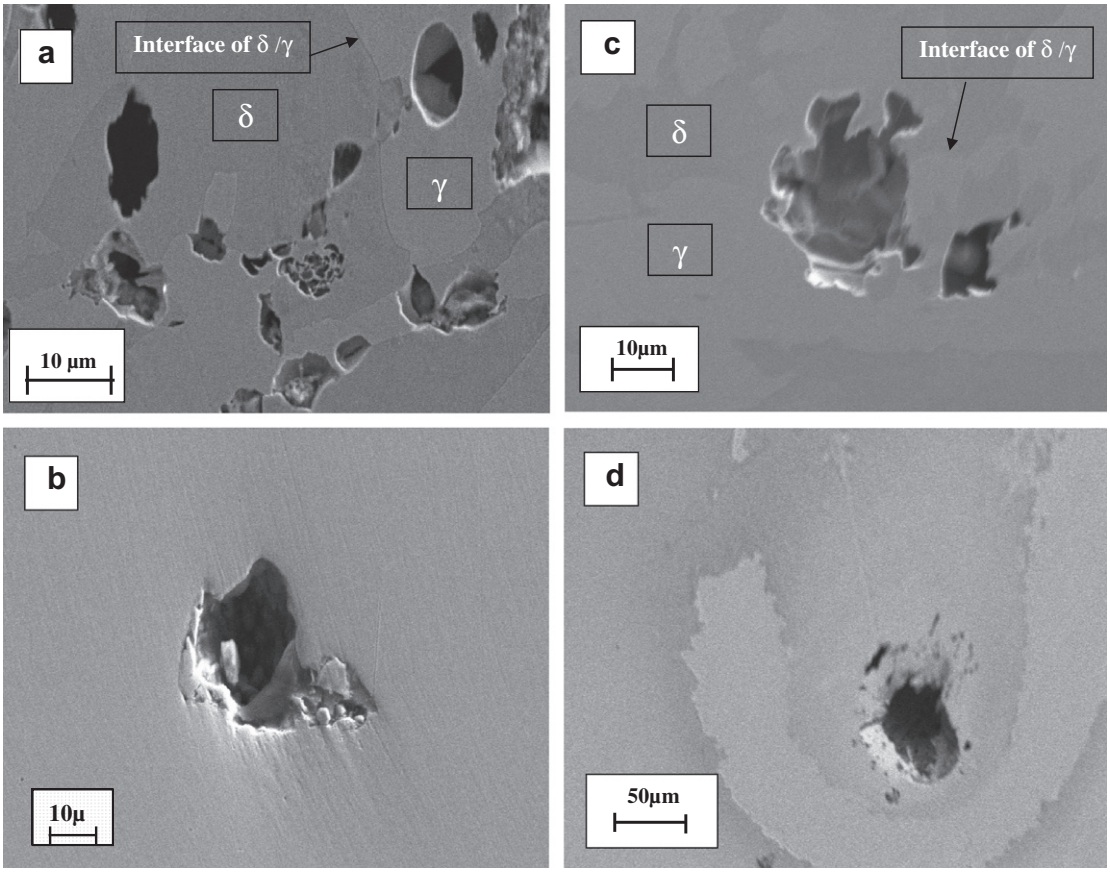


**Fig. 14.** Pit morphology of DSS 2205 after 850 mV potentiostatic polarisation above corrosion potential (a and b) in 0.1 M NaCl at 55 °C (c and d) in 0.1 M NaCl + 0.01 M $MoO_4^{2-}$ at 80 °C after and before etching, respectively.

depletion in austenite–ferrite interface and consequently the lower chromium content in austenite compared to ferrite phase or probably higher density of inclusions in this area.

## 4. Conclusion

The aim of this work was to study the influence of inhibiting effect of adding 0.0001, 0.001, 0.01 and 0.1 M molybdate ion on pitting corrosion and CPT of 2205 DSS in 0.1 M NaCl solution. The results can be summarized as follows:

(1) Addition of molybdate into the solution containing 0.1 M NaCl improves the critical pitting temperature of 2205 SS alloy. Based on the results of potentiodynamic polarisation CPT measurement, in the presence of 0.01 M molybdate ,the alloy CPT increased up to 10 °C and interestingly when the concentration of molybdate raised to 0.1 M, no evidence of pitting corrosion up to 85 °C was observed.
(2) Although the results of potentiostatic polarisation CPT measurement of the alloy were slightly higher than the results obtained from potentiodynamic polarisation techniques, a similar behaviour regarding the beneficial effect of molybdate on improving the alloy CPY was obtained. The alloy CPT was increased from 55 to 68 °C in 0.1 M NaCl. After 0.01 M molybdate ion was introduced into the solution, no pitting corrosion was observed up to 85 °C in the presence of 0.1 M molybdate in solution.
(3) Finally, pits morphology observed in chloride-containing solution after anodic polarisation indicates that the localized attacked seems to be associated to the interface between austenite and ferrite phases and propagates in austenite phase both in solution with and without molybdate inhibitor.

## Acknowledgement

Authors would like to appreciate the financial support from Ferdowsi University of Mashhad for providing the laboratory facilities during the period that this research was conducted.

## References

[1] A. Neville, T. Hodgkiess, An assessment of the corrosion behaviour of high-grade alloys in seawater at elevated temperature and under a high velocity impinging flow, Corros. Sci. 38 (1996) 927–956.
[2] B. Deng, Y. Jiang, J. Gong, C. Zhong, J. Gao, J. Li, Critical pitting and repassivation temperatures for duplex stainless steel in chloride solutions, Electrochim. Acta 53 (2008) 5220–5225.
[3] A. Igual Munoz, J. Garcia Anton, J.L. Guinon, V. Perez Herranz, Inhibition effect of chromate on the passivation and pitting corrosion of a duplex stainless steel in LiBr solutions using electrochemical techniques, Corros. Sci. 49 (2007) 3200–3225.
[4] A. Igual Munoz, J. Garcia Anton, J.L. Guinon, V. Perez Herranz, The effect of chromate in the corrosion behaviour of duplex stainless steel in LiBr solutions, Corros. Sci. 48 (2006) 4127–4151.
[5] A.M. do Nascimento, M.C.F. Ierardi, A.Y. Kina, S.S.M. Tavares, Pitting corrosion resistance of cast duplex stainless steels in 3.5% NaCl solution, Mater. Charact. 59 (2008) 1736–1740.
[6] V.S. Moura, L.D. Lima, J.M. Pardal, A.Y. Kina, R.R.A. Corte, S.S.M. Tavares, Influence of microstructure on the corrosion resistance of the duplex stainless steel UNS S31803, Mater. Charact. 59 (2008) 1127–1132.
[7] V. Muthupandi, P. Bala Srinivasan, S.K. Seshadri, S. Sundaresan, Effect of weld metal chemistry and heat input on the structure and properties of duplex stainless steel welds, Mater. Sci. Eng. A 358 (2003) 9–16.
[8] S.A. Tavara, M.D. Chapetti, J.L. Otegui, C. Manfredi, Influence of nickel on the susceptibility to corrosion fatigue of duplex stainless steel welds, Inter. J. Fatigue 23 (2001) 619–626.

[9] I.N. Bastos, S.S.M. Tavares, F. Dalarda, R.P. Nogueira, Effect of microstructure on corrosion behaviour of superduplex stainless steel at critical environment conditions, Script. Mater. 57 (2007) 913–916.
[10] G.O. Ilevbare, G.T. Burstein, The inhibition of pitting corrosion of stainless steels by chromate and molybdate ions, Corros. Sci. 45 (2003) 1545–1569.
[11] W.J. Tobler, S. Virtanen, Effect of Mo species on metastable pitting of Fe18Cr alloys – a current transient analysis, Corros. Sci. 48 (2006) 1585–1607.
[12] C.R. Alentejano, I.V. Aoki, Localized corrosion inhibition of 304 stainless steel in pure water by oxyanions tungstate and molybdate, Electrochim. Acta 49 (2004) 2779–2785.
[13] S.A.M. Refaey, Inhibition of steel pitting corrosion in HCl by some inorganic anions, Appl. Surf. Sci. 240 (2005) 396–404.
[14] S.A.M. Refaey, S.S. Abd El-Rehim, F. Taha, M.B. Saleh, R.A. Ahmed, Inhibition of chloride localized corrosion of mild steel by $PO_4^{3-}$, $CrO_4^{2-}$, $MoO_4^{2-}$, and $NO^{2-}$ anions, Appl. Surf. Sci. 158 (2000) 190–196.
[15] K. Sugimoto, Y. Sawada, Role of alloyed molybdenum in austenitic stainless steels in the inhibition of pitting in neutral halide solutions, Corrosion 32 (1976) 347–352.
[16] M.S. Vukasovich, J.P.G. Farr, Molybdate in corrosion inhibition – a review, Polyhedron 5 (1986) 551–559.
[17] ISO 17864: "Corrosion of Metals and Alloys – Determination of the Critical Pitting Temperature Under Potentiostatic Control", 2005.
[18] M.H. Moayed, N.J. Laycock, R.C. Newman, Dependence of the Critical Pitting Temperature on surface roughness, Corros. Sci. 45 (2003) 1203–1216.
[19] M.H. Moayed, R.C. Newman, Evolution of current transients and morphology of metastable and stable pitting on stainless steel near the critical pitting temperature, Corros. Sci. 48 (2006) 1004–1018.
[20] A. Pardo, M.C. Merino, A.E. Coy, F. Viejo, R. Arrabal, E. Matykina, Pitting corrosion behaviour of austenitic stainless steels – combining effects of Mn and Mo additions, Corros. Sci. 50 (2008) 1796–1806.
[21] B. Deng, Y. Jiang, J. Liao, Y. Hao, C. Zhong, J. Li, Dependence of critical pitting temperature on the concentration of sulphate ion in chloride-containing solutions, Appl. Surf. Sci. 253 (2007) 7369–7375.
[22] P. Ernst, R.C. Newman, Pit growth studies in stainless steel foils. II. Effect of temperature, chloride concentration and sulphate addition, Corros. Sci. 44 (2002) 943–954.
[23] M.H. Moayed, R.C. Newman, Aggressive effects of pitting "inhibitors" on highly alloyed stainless steels, Corros. Sci. 40 (1998) 519–522.
[24] M.H. Moayed, R.C. Newman, Deterioration in critical pitting temperature of 904L stainless steel by addition of sulfate ions, Corros. Sci. 48 (2006) 3513–3530.
[25] R.G. Kelly, J.R. Scully, D.W. Shoesmith, R.G. Buchheit, Electrochemical Techniques in Corrosion Science and Engineering, Marcel Dekker, Inc., New York, Basel, 2003.
[26] G.T. Burstein, Daymond, The remarkable passivity of austenitic stainless steel in sulphuric acid solution and the effect of repetitive temperature cycling, Corros. Sci. 51 (2009) 2249–2252.
[27] G.O. Ilevbare, G.T. Burstein, The role of alloyed molybdenum in the inhibition of pitting corrosion in stainless steels, Corro. Sci. 43 (2001) 485–513.
[28] P.I. Marshall, G.T. Burstein, Effect of alloyed molybdenum on the kinetics of repassivation on austenitic stainless steels, Corros. Sci. 24 (1984) 463–478.
[29] N.J. Laycock, M.H. Moayed, R.C. Newman, Metastable pitting and the critical pitting temperature, J. Electrochem. Soc. 145 (1998) 2622–2628.
[30] A.A.J. Aldykiewicz Jr., H.S. Isaacs, Dissolution characteristics of duplex stainless steels in acidic environments, Corros. Sci. 39 (1998) 516–535.